Analysis of the Power Load when Finishing Very Precise Holes by Reaming Head MT3

Josef Sedlak[1], Ales Jaros[1], Martin Slany[1], Karel Kouril[1], Jozef Majerik[2], Igor Barenyi[2]
[1]Department of Machining Technology, Institute of Manufacturing Technology, Faculty of Mechanical Engineering, Brno University of Technology, Technicka 2896/2, Brno 616 69, Czech Republic. E-mail: sedlak@fme.vutbr.cz, jaros.a@fme.vutbr.cz, slany.m@fme.vutbr.cz, kouril.k@fme.vutbr.cz
[2]Faculty of Special Technology, Alexander Dubcek University of Trencin, Pri Parku 19, Trencin 911 50, Slovakia. E-mail: jozef.majerik@tnuni.sk, igor.barenyi@tnuni.sk

Design and technological development of cutting tools represents a fluent process that combines new knowledge from all usable technical branches with actual needs and development results of component base, production technology and machine tools. The main factors which nowadays accelerate the development of cutting tools are constantly increasing demands to improve efficiency and productivity while reducing operation costs, the application of hard machinable materials, environmental protection issues, health and growing demands for greater safety. The article deals with methodology of measurement and evaluation of cutting forces and cutting torque at a special reaming head MT3 from FINAL Tools Inc. Solution of force loading during reaming by these modern tools enable to analyse the causes of cutting tool deficiencies starting from coating suitability up to weaknesses in their design. The article also analyses the significance of the reaming process from the reaming view point using a process liquid, including a tool life analysis combined with the tool wear.

Keywords: Reaming Head, MT3, Finishing, Precise Holes, Force Loading

1 Introduction

The main factors that nowadays accelerate development of the cutting tools are constantly increasing needs to efficiency rise and production productivity while reducing operation costs, application of hard machinable materials, environmental protection issue, health and increasing requirements on higher job safety [1], [2], [3], [4]. Authors Wang et al. [12] and Pilný et al. [16] realized their investigations with regards to the quality and reproducibility of reaming process. The reaming head MT3 is a productive tool for finishing very precise holes. The head is thermally clamped in the tool body. The thermal clamping provides reliable and precise setting of the reaming head without adjusting. Easy replacement of the head in the tool body is comparable with inserts in a tool holder what means also the same advantages – speed, simplicity and accuracy of the cutting tool exchange. The process liquid is supplied through the tool body not only to the individual cutting edge but around the whole head up to the guides. When reaming blind holes liquid is fed through the reaming head center. The geometry of the MT3 head is a new, patented original solution. The MT3 reaming head has 3 cutting edges and 2 guides. Optimal placement of cutting edges and guides around the head circumference provides support to edges when cutting and prevents vibration. Smooth tool motion has a positive influence on achieving process results, i.e. a roundness, cylindricity and surface finish. This solution also increases a lifetime even in comparison with more cutting edge tools [1], [2], [3], [4]. Company FINAL Tools Inc. has been working on development of modern reaming heads MT3 for many years and has been a significant specialist in this activity. The reaming head MT3 has a unique design of the reaming tool intended for finishing high precision holes in accuracy degrees IT5 to IT6 even while reaching high demands on shape, dimensional accuracy and surface roughness [1], [2], [3], [4].

2 Analysis of Force Stress Evaluation

Plunging of the reaming head MT3 into the cut is done in order displayed in Fig. 1. As the first cuts in the workpiece material the edge number 1 followed by the edges 2 and 3. Due to the spacing of cutting edges on only one half of the head circumference at the moment deflection from the tool axis and vibrations may occur. After all three edges are cutting the guides are involved into the process on the other half of the head circumference which stabilize the tool and push cutting edges into the cut. This sequence proceeds in a few microseconds, but at this stage there is an increase the reaming feed force components and cutting torque [1], [2], [3], [4].

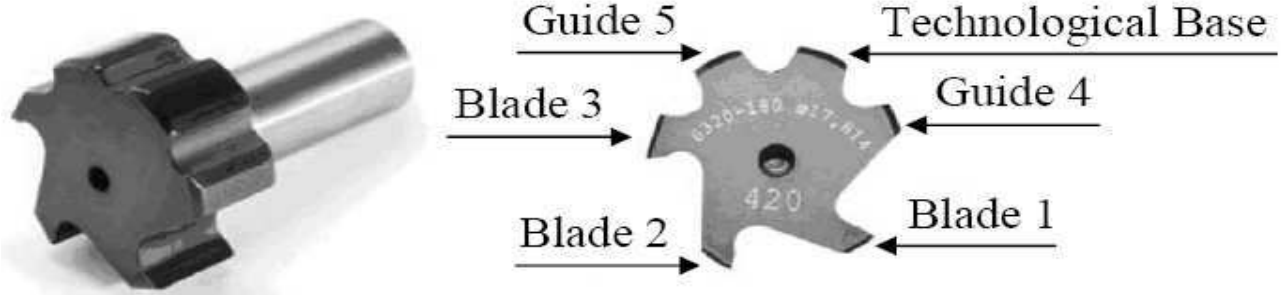

Fig. 1 *Reaming head MT3 [4]*

2.1 Evaluation of Force Stress During Machining

When machining, there is possible on the cutting tool to define two basic types of force components - active and passive. They are accompanying quantities of many mechanical technologies, during which the mechanically performed work is transformed [1].

During machining the load of the cutting tool is generated particularly by the workpiece resistance R against the cutting edge. The total force F exerted on the cutting tool may be expressed in different orientation of Cartesian coordinate systems. They are for example [1]:

- Coordinate System of Cutting Tool $\left(F_\gamma, F_{\gamma N}, F_p\right)$,
- Cartesian Coordinate System of Kistler Apparatus $\left(F_x, F_y, F_z\right)$,
- Coordinate System of Machine Tool $\left(F_x, F_y, F_z\right)$.

Active components of power load of cutting edge (F_c, F_f) are connected when machining with material removal (chip cross-section, specific cutting resistance or specific cutting force), cutting speed v_c and feed v_f. They participate in performances and activities connected with transformation of removal material into a chip [1]. The passive components of power load of cutting edge F_p during machining are such stresses at cutting tool that relates to the chip formation but since the tool does not move relatively in their direction the forces do not perform any work. They usually are components orthogonal to cutting speed v_c and feed v_f [1]. The total force F is thus decomposed into individual force elements [2] F_c, F_p, F_f, which may be determined from empirical relations (1 to 3) for the tool using during the cutting process a cutting wedge with defined geometry. The size of force load during machining process is in units [N]. General distribution of forces in reaming operation is in the Fig. 2. The cutting force F_c for the cutting tool with more edges – the reaming head MT3, results from a relation of measuring cutting resistance k_c [MPa] [3].

$$k_{ci} = \frac{F_{ci}}{A_{Di}} \text{ [MPa]} \tag{1}$$

$$F_{ci} = A_{Di} \cdot k_{ci} \text{ [N]} \tag{2}$$

The total cutting force is a vector sum of individual cutting forces generated by engaged cutting edges.

$$F_c = \sum_{i=1}^{z_z} A_{Di} \cdot k_{ci} \text{ [N]} \tag{3}$$

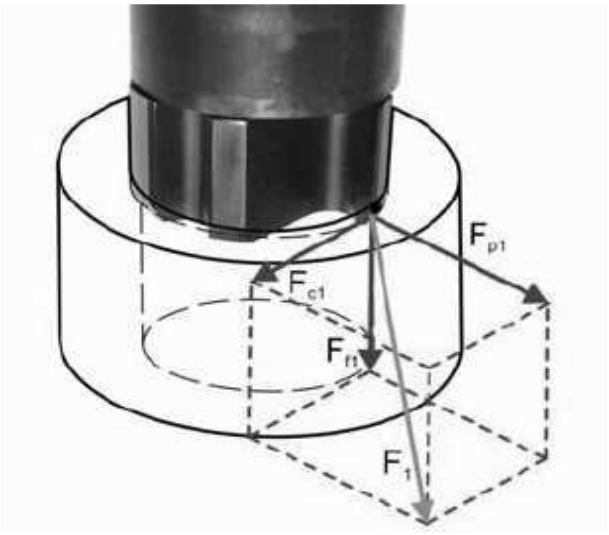

Fig. 2 *General distribution of force elements during reaming process [4]*

When machining, the creation and growth of wear in the form of facets occurs on the flank of the tool Fig. 3. This results in a change of the tool geometry and subsequently changes of the size and direction of the resulting force load, which is shown by changing the ratio of the individual force components. The passive force component F_p then may exceed the cutting force F_c and the feed force F_f up to three times. This change may be expressed as a function of time t in the orthogonal plane of cut by following relations (4 to 6) where the index h means a horizontal direction and v vertical one [2].

$$dF_h = \frac{\partial F_h}{\partial t} \cdot dt = \frac{\partial F_h}{\partial \gamma_o} \cdot d\gamma_o + \frac{\partial F_h}{\partial r_n} \cdot dr_n + \mu \cdot dF_v + \frac{\partial F_h}{\partial R_a} \cdot dR_a \tag{4}$$

$$dF_v = \frac{\partial F_v}{\partial t} \cdot dt = \frac{\partial F_v}{\partial VB} \cdot dVB + \frac{\partial F_v}{\partial r_n} \cdot dr_n \tag{5}$$

$$\frac{\partial^2 F_v}{\partial t^2} \cong 0 \quad \frac{\partial^2 F_h}{\partial t^2} \cong 0 \tag{6}$$

Where:

γ_o – orthogonal angle of rake [°],

r_n – rounding radius of cutting edge [mm],

μ – Newton-Coulomb coefficient of friction [-],

VB – size of the wear on the tool flank [mm],

t – time [s].

The following relations are applied for stabilized machining:

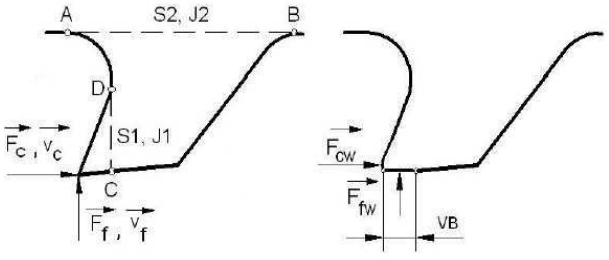

Fig. 3 *Schematic representation of planar stress of tool cutting edge (on the left – sharp tool; on the right – worn tool on the rake and flank) [4]*

Part of the work is determination of the size of force load and torque generated by the cutting edges of reaming head MT3 during the approach of tools into the cut of the hole in the test sample. For measuring the force load and cutting torque, the piezoelectric quartz Kistler dynamometer 9272 located on five-axis CNC vertical machining center MCV 1210 Fig. 4, which is part of workshop C2 at Institute of Manufacturing Technology, Faculty of Mechanical Engineering, Brno University of Technology had been used. Authors Dubovská et al. [15] also realized similar investigations and measurement of cutting forces during the machining process.

Fig. 4 *Scheme of measurements using piezoelectric dynamometer Kistler 9272 placed on 5-axis CNC machining centre MCV 1210*

A calculation of the cutting force proceeds from an equation (2). However, this equation does not include an influence of the tool wear on the force load. The equation considering wear of the tool must be thus supplemented by a component $F_{c\omega}$ as indicated in equation (7) to (10). Other components of the power load provide relations (11) and (12) [3], [4].

$$F_c = F_{co} + F_{c\omega} [\mathrm{N}] \tag{7}$$

$$F_{co} = A_D \cdot k_c = a_0 [\mathrm{N}] \tag{8}$$

$$F_{c\omega} = a_1 \cdot t + a_2 \cdot t^2 [\mathrm{N}] \tag{9}$$

$$F_c = a_0 + a_1 \cdot t + a_2 \cdot t^2 [\mathrm{N}] \tag{10}$$

$$F_p = k_{Fp}(t) \cdot F_c [\mathrm{N}] \tag{11}$$

$$F_f = k_{Ff}(t) \cdot F_c [\mathrm{N}] \tag{12}$$

Where:

F_{co} – cutting force component of unworn edge – new tool [N],

$F_{c\omega}$ – cutting force component of worn cutting edge [N],

A_D – chip section [mm^2],

k_c – specific cutting resistance [MPa],

k_{Fp} – coefficient for calculation of passive force component [-],

k_{Ff} – coefficient for calculation of feed force component [-].

Analogically, to express the total cutting torque M_{ctot} (13) by a relation (7) it is necessary to include components $M_{c\omega}$ and M_{Gp}. For the new tool the torque $M_{c\omega}$ will be considered as a zero. The value of the cutting torque M_c is given by a relation (14) [3], [4].

$$M_{ctot} = M_c + M_{c\omega} + M_{Gp} \ [\mathrm{N.m}] \tag{13}$$

$$M_c = F_c \cdot r \ [\mathrm{N.m}] \tag{14}$$

3 Experimental Research

In the course of solving given problems, the analysis of workpiece material, the coating morphology and measurement of force load and cutting torque were performed.

3.1 Machined Material

The workpiece material is a heat-rolled steel 15 260.7 (DIN 50CrV4) hardened to 30±1 HRC. Mechanical, physical and chemical properties of the workpiece material are shown in Tab. 1 (all measurement were realized in FST TnUAD Trencin and Tab. 2 (measured with the measuring device Spectrolab JrCCD in Trenčín). Structure of the workpiece material, see in Fig.5 tempered martensite, carbide-fine dispersion of secondary carbides, residual austenite and inclusions (oxidic and MnS type) [5]. Thirty samples of diameter 29 mm to 15 mm were tested, which can see in Fig.6. Heat treatment: tempered steel – tensile strength R_m = 885 up to 1030 MPa.

Tab. 1 *Nominal properties of the workpiece material (Mn-Cr-V steel for refining)*

Mechanical Qualities				
Yield Stress Re_{min} [MPa]	**Tensile Strength R_m [MPa]**	**Hardness [HRC]**	**Modulus of Elasticity E [GPa]**	**Modulus of Shear Elasticity G[GPa]**
735	885 up to 1030	30±1	215.7	83.3

Physical Qualities			
Specific Weight ρ [kg·m^{-3}]	**Thermal Expansion Coefficient α [K^{-1}·10^{-6}]**	**Thermal Conductivity λt [W·m^{-1}·K^{-1}]**	**Resistivity ρ [Ω·m·10^{-6}]**
7.850	12	41	190

Tab. 2 *Workpiece material (Mn-Cr-V steel for refining)*

Steel	**Chemical Composition [wt. %]**								
	C	**Mn**	**Si**	**Cr**	**V**	**Ni**	**P**	**S**	**Fe**
15 260 (~DIN50CrV4)	0.47-0.55	0.70-1.00	0.15-0.40	0.90-1.20	0.10-0.20	Max. 0.30	Max. 0.035	Max. 0.035	Rest

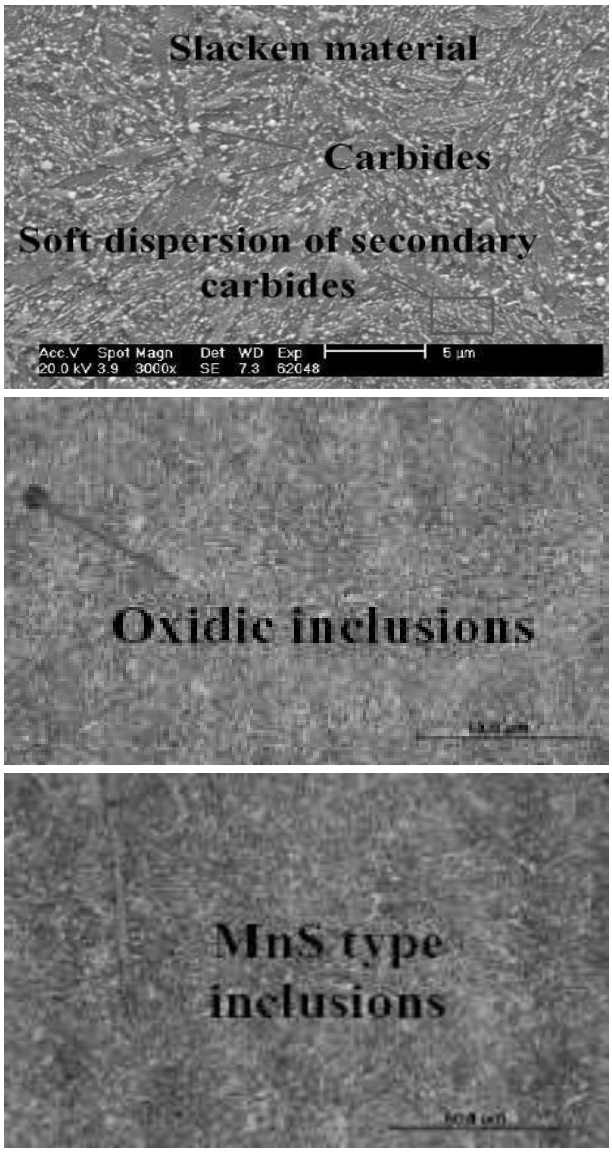

Fig. 5 *Structure of workpiece material (tempered martensite, carbides + fine dispersion of secondary carbides, residual austenite and inclusions – oxidic and MnS type). Nital 2%*

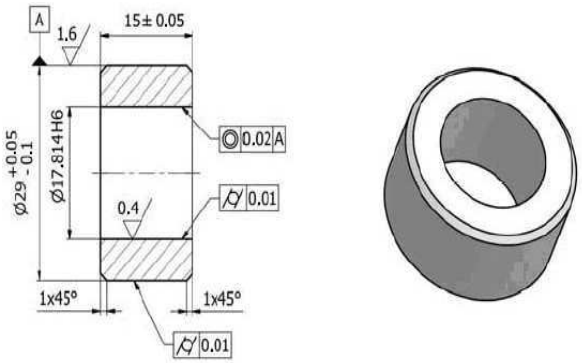

Fig. 6 *Tested Sample [4]*

For evaluation of the workpiece material (steel 15 260.7) light and electron microscopy were used and obtained pictures applied for an image analysis. Structure evaluation is realized by a light microscope OLYMPUS GX 51 with a digital camcorder [5]. The same observations have been realized by the authors Pokorný et al. [13].

Machining of the material 15 260.7 was implemented, without the process liquid, force load and the cutting torque, using short-term tests. During the reaming process using the tool MT3, the process liquid, which is fed through the tool body not only to individual edges, but across the whole head periphery up to the guides, is usually used. During reaming of blind holes the liquid is fed through the middle of the reaming head MT3 [5].

3.2 Clamping Fixture

Individual samples were clamped by a special jig (can be seen in Fig. 7), which was made specifically for this purpose – reaming with MT3 head. Tested samples are clamped to the fixture to eliminate body deformation during clamping around the periphery [4].

Fig. 7 *Special fixture for clamping tested samples [4]*

3.3 Applied Cutters

For the experimental part, the modern reaming head MT3 patented by company FINAL Tools Inc., was chosen, see Fig. 8. The tools of this type are usually monolithic or soldered. The tools are provided with three cutting edges and two guides. The area between guides serves as a technological base for checking and measuring the reamer diameter. The toleration field of reamed hole is according to a producer within range IT5 to IT6. Surface roughness after the reaming operation reaches value up to $Ra=0.4\mu m$[6], [7].

In Tab. 3, there is a list of all tools applied, including their cutting conditions that were used for production of the hole in required accuracy and surface finish. For production of the hole the following technological operations were used, their number match the tool number specified in Tab. 3 [8], [9].

Fig. 8 *Reaming head MT*

Tab. 3 *Cutting conditions used for individual cutting tools [9]*

Cutting Conditions					
Tool No.	**Cutting speed v_c [m.min^{-1}]**	**Revolutions n [min^{-1}]**	**Feed f [mm]**	**Feed rate v_f [mm.min^{-1}]**	**Cooling**
1.	35	2,500	0.05	125	YES External Cooling
2.	35	1,390	0.1	139	
3.	35	700	0.15	110	
4.	60	1,100	0.1	110	
5.	60; 80; 100; 120	1,100; 1,430; 1,790; 2,146	0.42	462 up to 900	No

1. Sinking (center drill ø1.5 x 60° DIN 333A HSS),
2. Drilling (drill DIN 338 HSS Co ø8 mm),
3. Hole extension by drilling (drill SK M44 ø17 mm),
4. Boring (boring bar HF with the CCMT 060204 cutting insert geometry ø17.7 mm +0.05 mm),
5. Reaming (reamer MT3 ø17.814 mm).

3.4 Analysis of Coating on the Reaming Head MT3

The reaming head MT3 is provided with a coating HSN^2 (a nanocomposite triple-layer coating $TiAl_xN$ of second generation), which is product of company CemeCon Ltd.. A suitability of the coating for the given applications is verified by long-term tests performed in research contracts awarded by FINAL Tools Inc. [5], [6], [7], [8], [9]. The coating was applied on the tool by the method of magnetron sputtering, using a system CC800/9ML. The temperature during the layer deposition was between values 450 to 480 °C. The coating thickness was verified by Kalotest (see in Fig. 9) and its value was 3.0 ± 1 μm. A nominal characteristic of the coating HSN^2 is given in Tab. 4 [5], [6], [7], [8], [9].

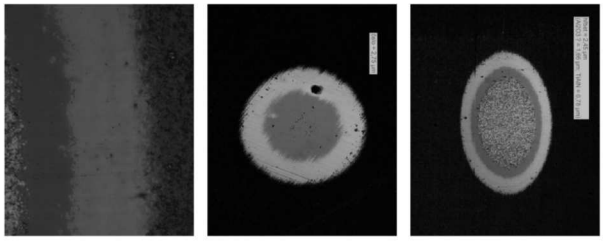

Fig. 9 *Pictures of calotte of HSN^2 coating at face and flank of reaming head MT3 [5], [6], [7], [8], [9]*

Tab. 4 *Nominal characteristic of HSN^2 coating [5], [6], [7], [8], [9]*

Cover	Group	Composition	Structure	Hardness [HV 0.05]	Max. Working Temperature [°C]	Friction Coefficient [-]
HSN^2	Super Nitride	$TiAl_xN$	Nanocomposite	3,800	1,100	0.3

The HSN^2 coating exhibits a high degree of hardness and simultaneously maximum resistance which is given by the nanocomposite structure. Using electron microscopy, SEM, morphology of the coating was observed. It has been demonstrated that the analyzed coating has a compact structure, non-porous and uniform interface, which results in very good adhesion. The morphology of the coating surface was observed with a scanning electron microscope PHILIPS X L30 [5], [6], [7], [8], [9].

4 Experimental Measurement and Results

To record a force load, measuring equipment with piezoelectric Kistler dynamometer with the type designation 9272 connected to an eight-channel amplifier Kistler

hub 5070 was used. During the experimental measurement, the data files of feed force F_f and the cutting moment M_c were gained. These values are plotted in a graphic function of time *t*. The Fig. 10 shows the typical course of reamer load. The progress is accompanied by initial and final peaks [9], [10], [11]. Due to the reduction of so-called anti-aliasing, the recording frequency is set to eight times greater than the selected RPM, in order to meet the Nyquist stability criterion measurements (15) [4].

$$\int(x)\cdot g(x)=\int_{-\infty}^{\infty} f(t)\cdot g(x-t)dt \qquad (15)$$

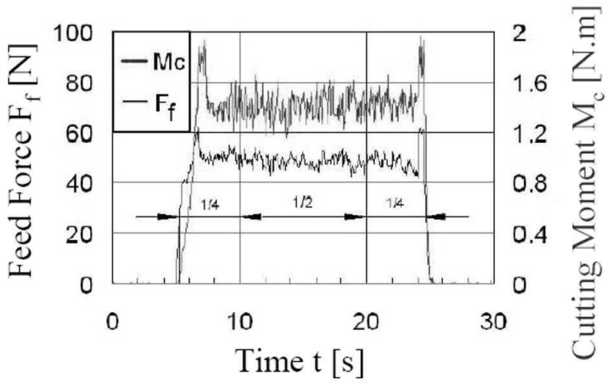

Fig. 10 *Course of load recorded for feed force component F_f and cutting torque M_c vs. time t during reaming operation [9]*

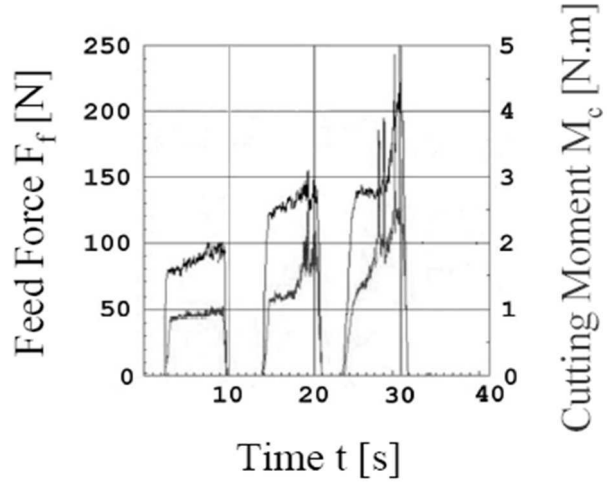

Fig. 11 *Growth of feed force component F_f and cutting torque M_c during testing of reaming head [9]*

The Fig. 11 shows that during the reaming process, the monitored feed force component and the cutting torque increase. Within the first measurement, the feed force component and the cutting torque are relatively stable. However, with every other measurement peaks occur in the course of feed force which is probably caused by adhesion of the machined material to the tool guides [9], [10], [11].

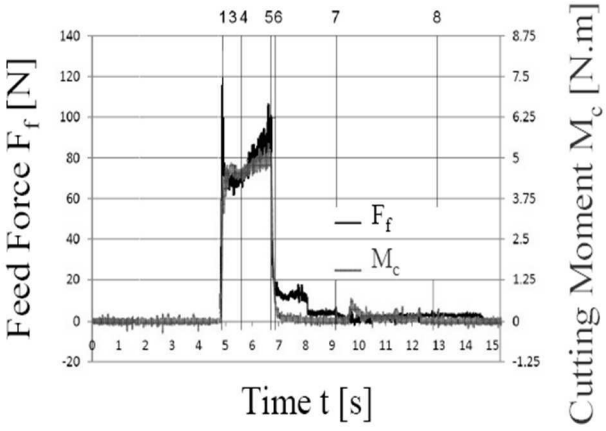

Fig. 12 *Graphical dependence of force load during reaming by head MT3 with indication of individual areas [9]*

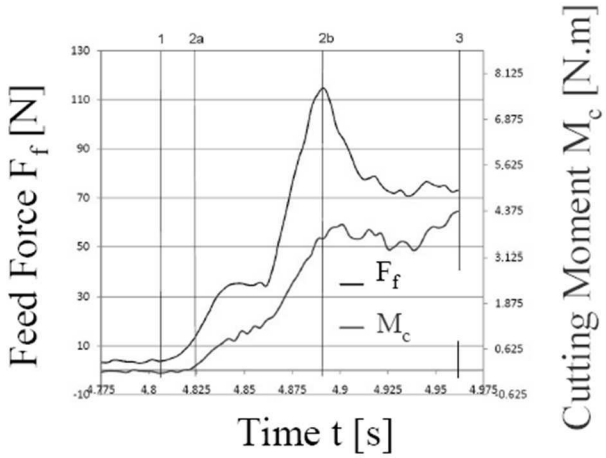

Fig. 13 *Detailed analysis of areas to 3 [9]*

Analysis of the feed force is displayed in Fig. 12, while the individual areas are described in more detail in Tab. 5. The detailed analysis of area determined by numbers 1 to 3 is made in a plot of Fig. 13, especially because of a very short time sequence of running processes associated with the beginning of cutting [9], [10], [11].

Tab. 5 *Description of individual areas of force load and analysis of running processes [9]*

Area Number	Ongoing Process
0-1	Delay before start of entry of first edge to cut
1-2	Entry of first blade to cut and follow-up connection of two remaining edges
2-3	Contact of guides with surface, connection of calibration part of tool
3-4	Full transmission of tool
4-5	Start of first edge leaving from transmission
5-6	Exit of remaining edges from transmission
6-7	Exit of remaining part of reamer from transmission
7-8	Slide reverse and leaving the finished hole

In the graphical dependence of Fig. 13 there is displayed the detailed progress of the feed force F_f and the cutting torque M_c in relation to time t. In the area 1 to 2a there emerge the beginning of the transmission of the first edge of reaming head MT3 and subsequently there appears transmission of other two edges. In the area determined by numbers 2a to 2b, there riseing chip cross-section taken away by all edges of reaming head. In the area 2b up to 3 the process is stabilized, which means that both guides touched the surface at the same time. The calibration part of the tool joins the reaming process [9], [10], [11]. During the experimental testing the wear of the reaming head MT3 was also evaluated. Examples of flank wear of the reaming head MT3 are displayed in Fig. 14, while the wear values are mentioned in the individual figures [9]. Authors Majerík et al. [14] realized experiments of the flank wear mechanisms which respect to a fact that with increasing of cutting speed, the oxidation wear on the flank face affects more highly.

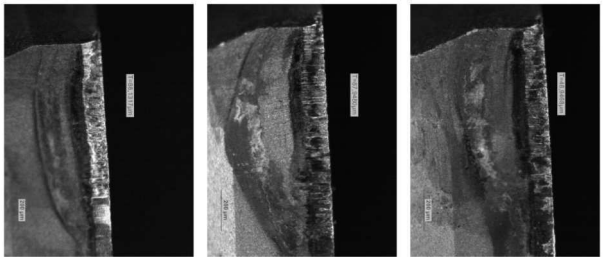

Fig. 14 *Examples of flank wear of reaming head MT3 with coating HSN² [9]*

In the Fig. 15 there are displayed plots of flank wear, wear of guide and head of the tool whereas in the figure which displays the tool guide of the reaming head MT3, there is a visibly recognizable adhesive adhesion of the machined material [9].

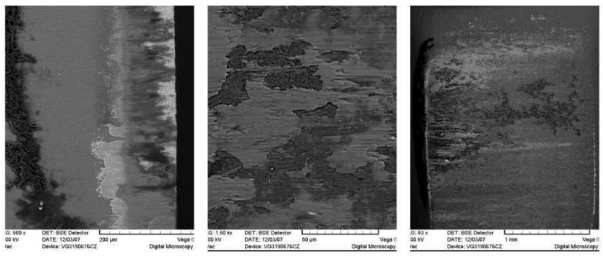

Fig. 15 *Wearing example of backs, guides and head of reaming head tool MT3 [9]*

5 Conclusion

In production of reaming holes high demands on dimension and shape accuracy of the produced hole are set. The other observed parameter is quality and surface finish of machined surface. Achieving the above-mentioned requirements depends on usage of quality reamers having especially high reliability.

All tools (the drill, boring bar and reaming head MT3) used for realization of the given issue have been borrowed from company FINAL Tools Inc. For the experiment, the reaming head MT3 with the coating HSN² – the nano-composite triple-layer coating $TiAl_xN$ of the second generation has been chosen. The coating has been applied by a physical method PVD.

The reaming head MT3 is heat-clamped to the tool body. The heat-clamping provides a reliable and accurate setting up of the reaming head MT3 without a necessity of the further adjusting. The simple replacement of the reaming head MT3 in the tool body is comparable with the replaceable edge plate in the tool holder. This way of clamping also brings the same advantages in form of speed, simplicity and accuracy of the replacement of the tool cutting part. Smooth running of the tool has a positive influence on reached results of the machining, i.e. the circular shape, cylindricity and the quality of the machined surface. This solution also prolongs lifetime in comparison with more-edged tools.

The material 15 260.7 has been used for the testing. It has been machined without the process liquid. Subsequently, it has been evaluated by short-time tests of their force load and the cutting torque.

During the reaming process the monitored feed force component and the cutting torque were rising. During the first measurement, the feed force and cutting torque were quite stable. With the following measurements, the peaks appeared during the force load. They probably were caused by adhesion of the machined material to the tool guides. During the experimental testing the wear of the reaming head MT3 was evaluated.

Acknowledgement

This article was supported and co-financed from a specific research FSI-S-16-3717 called "Research in Field of Modern Production Technologies for Specific Applications". This work was also supported by the Slovak Research and Development Agency under the contract No. APVV-15-0710.

References

[1] PÍŠKA, M., SLANÝ, M., MADAJ, M., POLZER, A. (2010). *Influence of Process Liquids on Active and Passive Force Elements during Drilling (in Czech).* Praha: Czech Engineering Society, 2010. ISBN 978-80-02-02237-4.

[2] ZOUHAR, J. (2009). Development of Efficient Milling Machines with Use of CAD/CAM and Analysis of Mechanism of Chip Formation (in Czech). Brno 2009. *Doctoral Thesis*. Brno University of Technology, Faculty of Mechanical Engineering, Department of Machining Technology. p. 104, 7 appendices. Thesis Supervisor doc. Ing. Miroslav Píška, CSc.

[3] FOREJT, M., PÍŠKA, M. (2006). *Theory of Machining, Shaping and Tools (in Czech).* Brno: CERM, 2006. ISBN 80-214-2374-9.

[4] SLANÝ, M. (2013). Study of Effects of Passive Force Cutting Elements on Machined Surface (in Czech). Brno 2013. *Dissertation Thesis*. Brno University of Technology, Faculty of Mechanical

Engineering, Department of Machining Technology. p. 137, 1 appendix. Thesis Supervisor prof. Ing. Miroslav Píška, CSc.

[5] FOREJT, M., SIZOVÁ, A., SEDLÁK, J. (2010). Analysis of Modern Grooving Methods using CNC Machines (in Czech). Brno: CERM, 2010. ISBN 978-80-214-4116-3.

[6] KOUŘIL, K., FIALA, S. *Modern Tools for Holes Finishing (in Czech).* 2007, pp 42-43, [online]. [seen 2017-03-10]. Available at: <http://www.mmspektrum.com/clanek/moderni-nastroje-pro-dokoncovani-der>.

[7] FIALA, S., KOUŘIL, K. *Cermet Reamers with Chip Formers (in Czech).* 2016, pp 116-117, [online]. [seen 2016-09-21]. Available at: <http://www.mmspektrum.com/clanek/cermetove-vystruzniky-s-utvareci-trisky.html>.

[8] OE217 – EUREKA. *Development and Innovation of Tools and Technologies for Finishing of Accurate Holes (in Czech).* Brno 2006. (2006 to 2008, MSM/OE Czech republic). Solver: Stanislav Fiala.

[9] SEDLÁK, J. et al. (2011). *Evaluation of Feed Force Progress during Reaming of holes by MT3 Head and Modelling of its Movement Kinematics (in Czech).* Brno 2011. Brno: Brno University of Technology, Faculty of Mechanical Engineering, Department of Machining Technology, p. 32. Final Report about Project Realization: Network to Support Cooperation among Technically and Business Oriented Universities with Companies in South Moravian Region CZ.1.07/2.4.00/12.0017.

[10] KOUŘIL, K. (2006). Finishing Operations of Reaming (in Czech). *MM Industry Spectrum,* 2006, Vol. 2006, No. 6, pp 32-33. ISSN 1212-2572.

[11] FIALA, S., KOUŘIL, K., ŘEHOŘ, J. (2015). Modern Technology of Finishing of Very Accurate Holes by Reaming and its Influence on Practical Qualities of Products (in Czech). *Manufacturing TECHNOLOGY,* 2015, Vol. XX, No. 1, pp 17-22. ISSN 1211-4162.

[12] WANG, Y., YANG, X., XU, Q. (2017). Study on cutting force and hole quality of PCD step reamer for reaming ZL102 alloy in dry and wet conditions. *International Journal of Advanced Manufacturing Technology,* 2017, Vol. 90, No. 5-8, pp 1693-1702. DOI: 10.1007/s00170-016-9503-6.

[13] POKORNÝ, Z., HRUBÝ, V., STUDENÝ, Z. (2016). Effect of nitrogen on surface morphology of layers. *Metallic Materials,* 2016, Vol. 54, No. 2, pp 119-124. DOI: 10.4149/km 2016 2 119.

[14] MAJERÍK, J., BARÉNYI, I. (2016). Experimental investigation into tool wear of cemented carbide cutting inserts when machining wear resistant steel Hardox 500. *Engineering Review,* 2016, Vol. 36, No. 2, pp 167-174. ISSN 1849-0433.

[15] DUBOVSKÁ, R., MAJERÍK, J. (2015). Experimental investigation and analysis of cutting forces when machining X5CrNi18-10 stainless steel. *Manufacturing TECHNOLOGY,* 2015, Vol. 2015, No. 3, pp 322-329. ISSN 1213-2489.

[16]PILNÝ, L., MÜLLER, P., DE CHIFFRE, L. (2014). Reproducibility of a reaming test. *International Journal of Manufacturing Research,* 2014, Vol. 9, No. 2, pp 157-172. DOI: 10.1504/IJMR.2014.062441.

10.21062/ujep/157.2018/a/1213-2489/MT/18/4/659